Electronic Supplementary Information
This journal is © The Royal Society of Chemistry 2021

Electronic Supplementary Information

Selenium-induced $NiSe_2$@$CuSe_2$ hierarchical heterostructure for efficient oxygen evolution reaction

Ting Li, Qing Zhang, Xiao Hu Wang, Juan Luo, Li Shen, Hong Chuan Fu , Fei Gu, Nian Bing Li*, Hong Qun Luo *

School of Chemistry and Chemical Engineering, Southwest University, Chongqing 400715, People's Republic of China

E-mail address: linb@swu.edu.cn (N. B. Li); luohq@swu.edu.cn (H. Q. Luo)

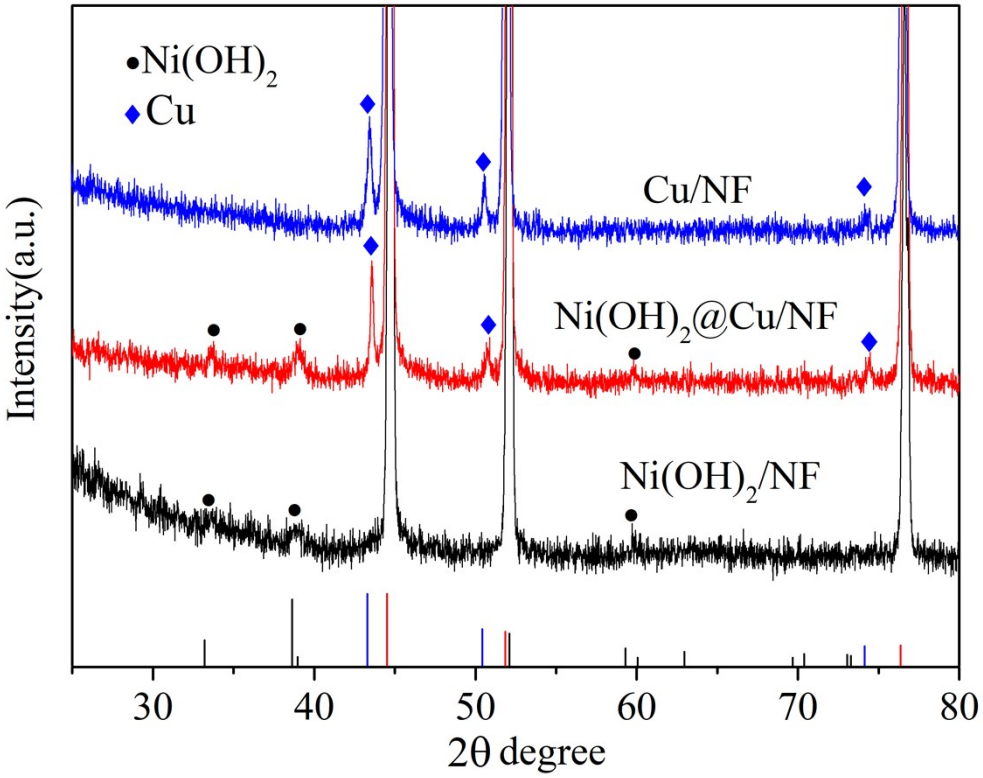

Fig. S1. XRD pattern of $Ni(OH)_2$@Cu/NF, $Ni(OH)_2$/NF and Cu/NF.

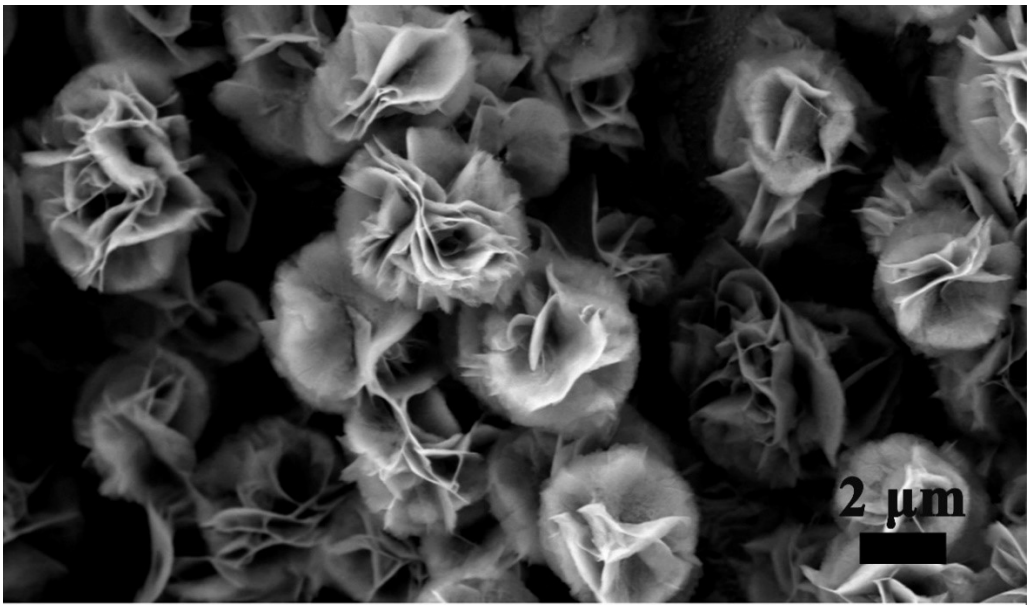

Fig. S2. SEM image of $Ni(OH)_2$@Cu/NF.

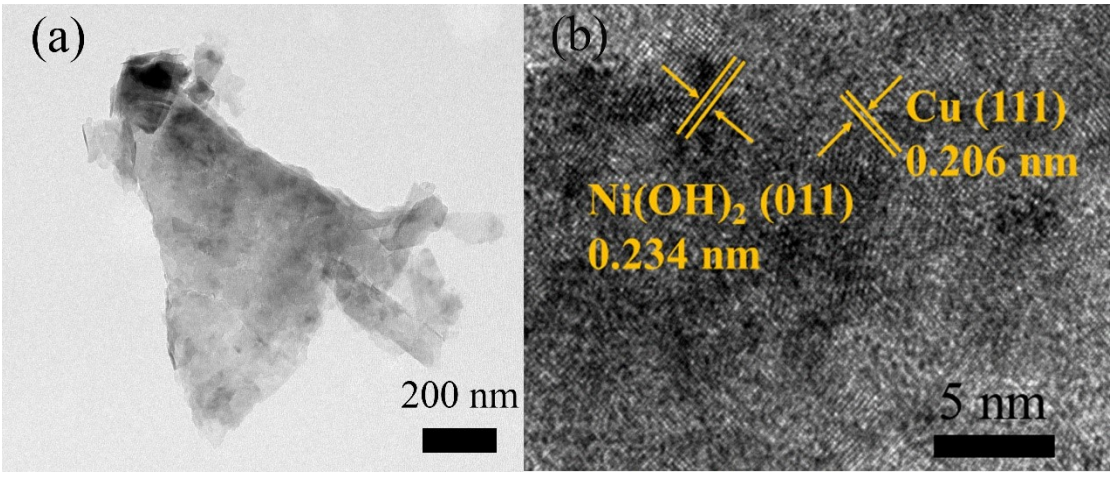

Fig. S3. a) TEM and b) HRTEM images of $Ni(OH)_2$@Cu.

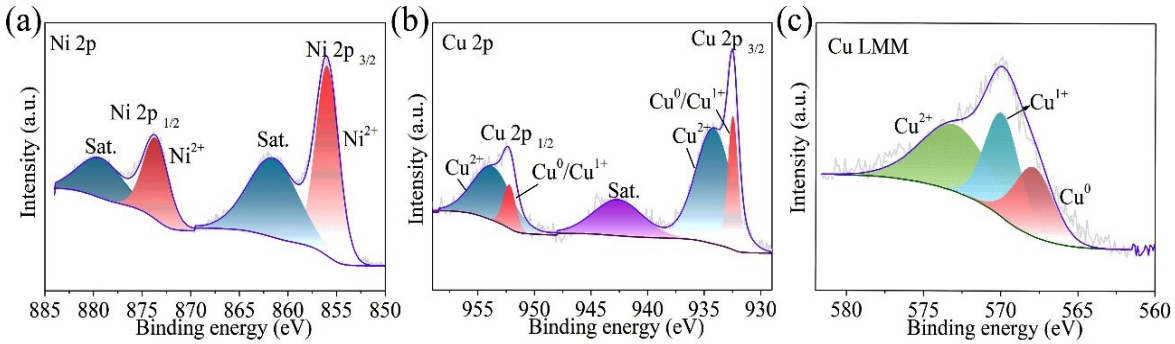

Fig. S4. The high-resolution XPS spectra of a) Ni 2p, b) Cu 2p, and c) Cu LMM for $Ni(OH)_2$@Cu.

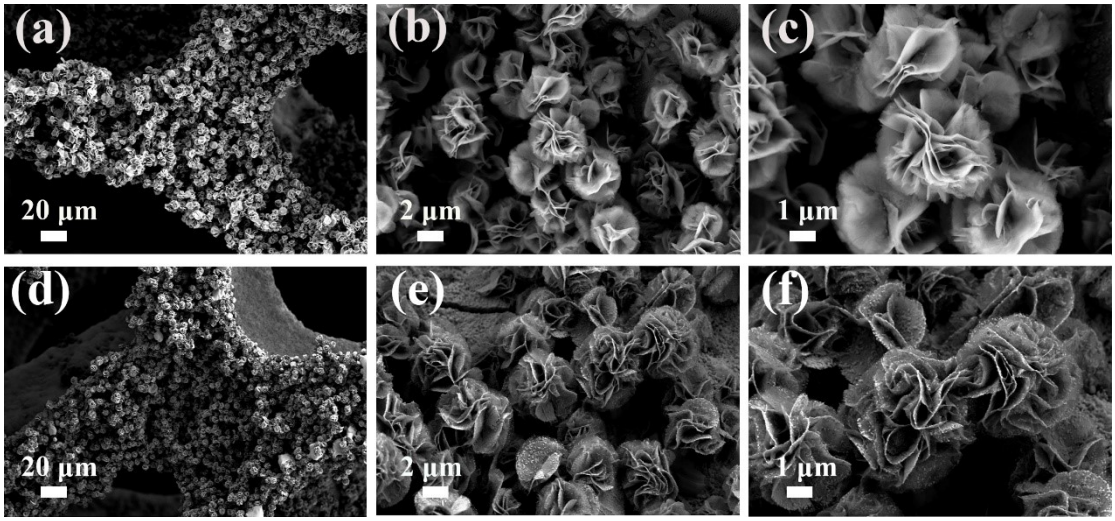

Fig. S5. SEM and magnified SEM images of a-c) $Ni(OH)_2$@Cu/NF, d-f) $NiSe_2$@ $CuSe_2$/NF.

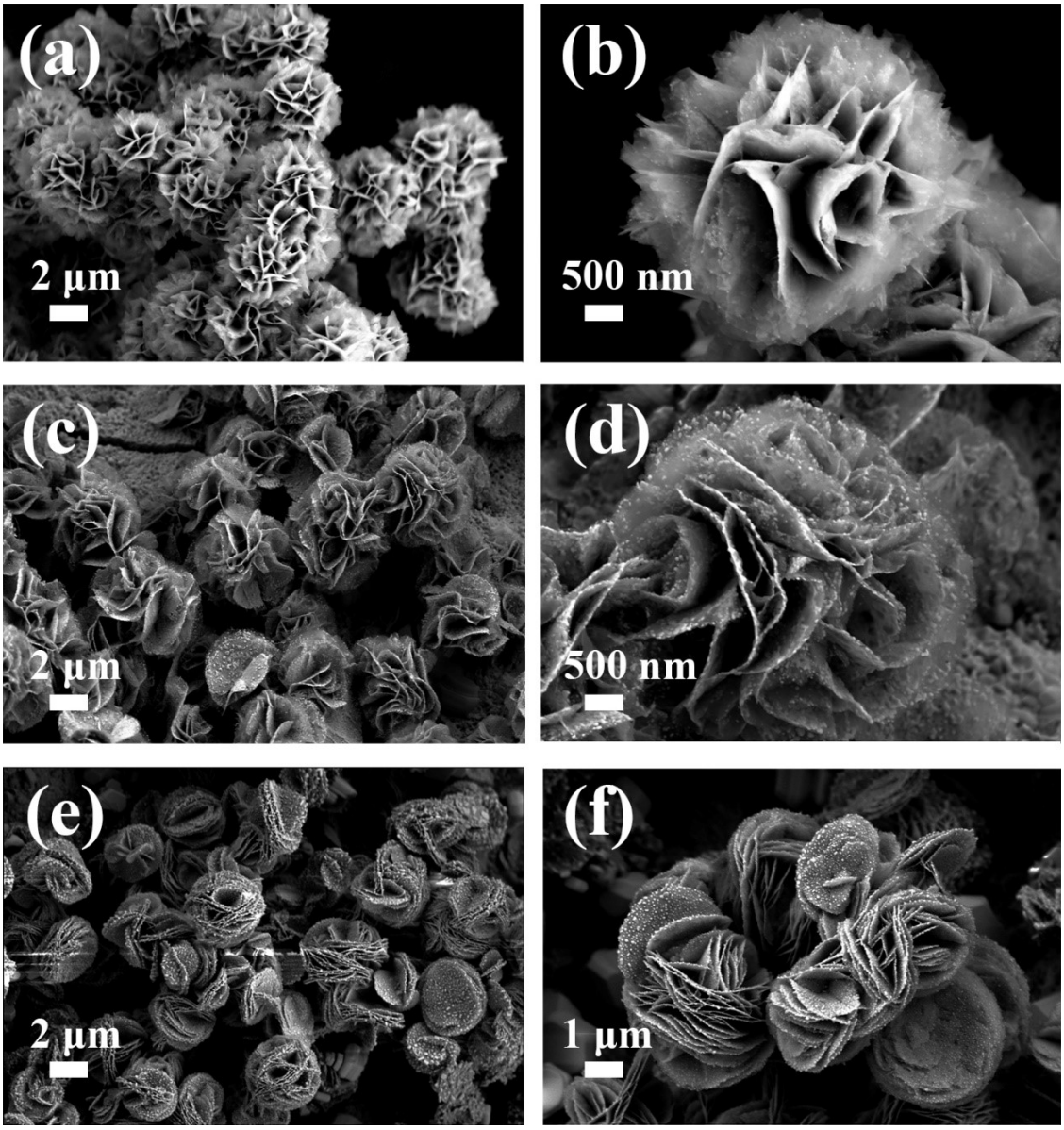

Fig. S6. SEM and magnified SEM images of a-b) NiCuSe-NF-0.1, c-d) NiCuSe-NF-0.2 e-f) NiCuSe-NF-0.3 (0.1, 0.2, 0.3 represent the ratio of nickel salt to copper salt).

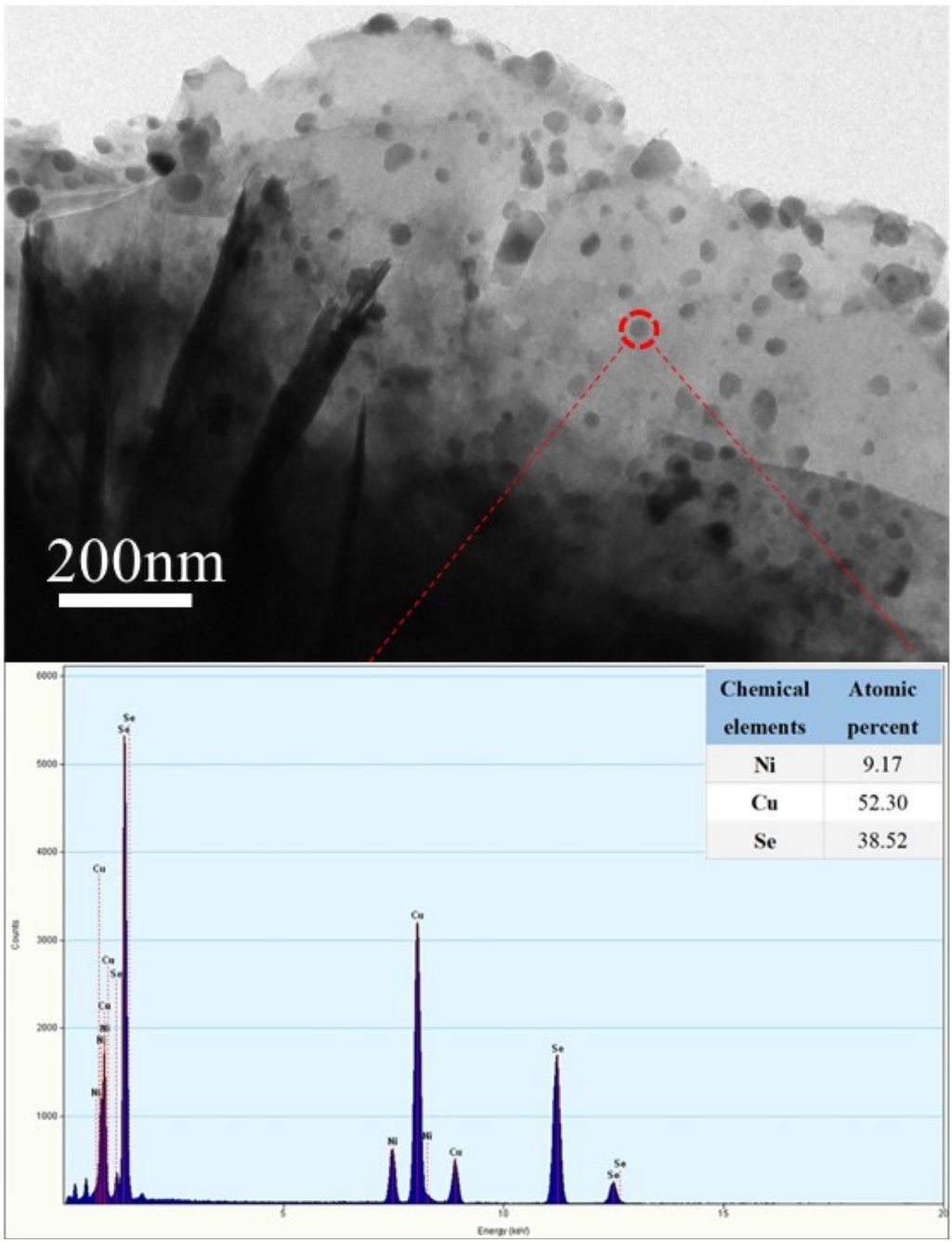

Fig. S7. EDS-point data of $NiSe_2$@$CuSe_2$/NF. Inset image is a table of atomic percent of Ni, Cu and Se.

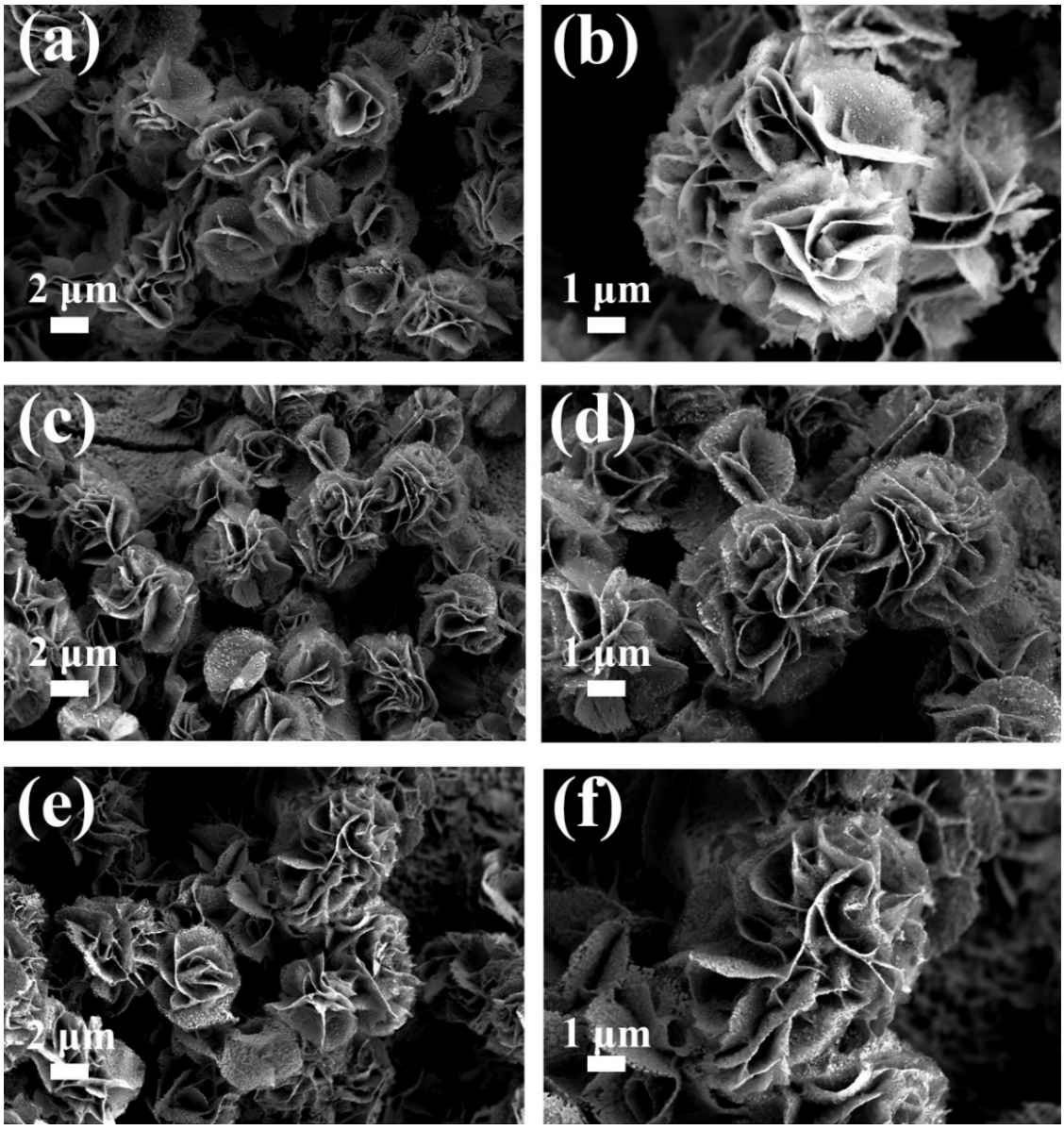

Fig. S8. SEM and magnified SEM images of $NiSe_2$@$CuSe_2$/NF with different hydrothermal time a-b) 3 h, c-d) 6 h e-f) 9 h.

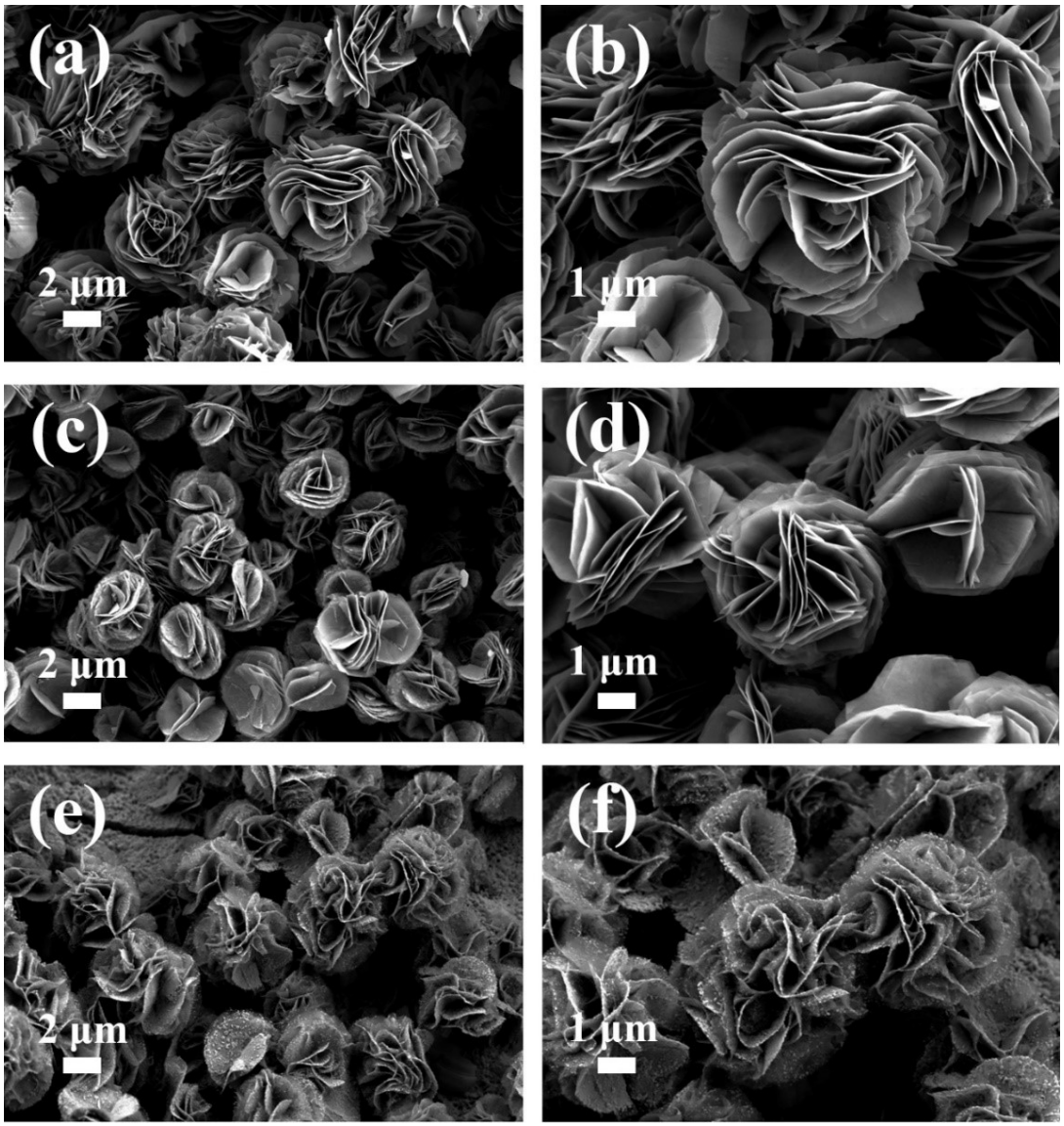

Fig. S9. SEM and magnified SEM images of $NiSe_2$@$CuSe_2$/NF at different hydrothermal temperatures: a-b) 120 °C, c-d) 160 °C , and e-f) 200 °C .

Table S1. Comparison of activity for OER of electrocatalysts in 1.0 M KOH.

Electrocatalyst	η for OER at target j (mV @ mA cm^{-2})	Substrate	Ref
$NiSe_2$	301@40	Carbon cloth	1
CuSe	382 @100	Ni foam	2
$CuCo_2Se_4$	320 @50	Au-coated glass	3
NiP_2@$NiSe_2$	329 @100	Carbon fiber	4
$Ni_{1.9}Cu_{0.1}$-S	259 @10	Ni Foam	5
NiFeSe@NiSe|O	360@100	Carbon cloth	6
P-$NiSe_2$@N-CNTs/NC[a]	407@100	Glassy carbon electrode	7
$Ni_{59}Cu_{19}P_9$	293@10	Cu foil	8
NC–NiCu–NiCuN	295@100	Ni foam	9
$NiSe_2$–$CoSe_2$	250@10	Ni–Co foam	10
Cu_3Se_2@$CoSe_2$–$NiSe_2$	240@10	Ni–Co foam	11
$CoSe_2$	280@10	Glassy carbon electrode	12
$Co_{0.9}Fe_{0.1}$-Se	287@100	Ni foam	13
FeCoMo-Se	264@10	Carbon cloth	14
Fe-doped $NiSe_2$	279@10	Glassy carbon electrode	15

[a] N-CNTs/NC denotes hierarchical N-doped carbon frameworks.

Table S2. The fitting results of EIS spectra in 1 M KOH for the OER.

Sample	R_s (ohm)	R_{ct} (ohm)
$NiSe_2$@$CuSe_2$/NF	2.817	1.998
$NiSe_2$/NF	2.948	5.130
$CuSe_2$/NF	3.199	42.54
$Ni(OH)_2$@Cu/NF	3.588	54.90

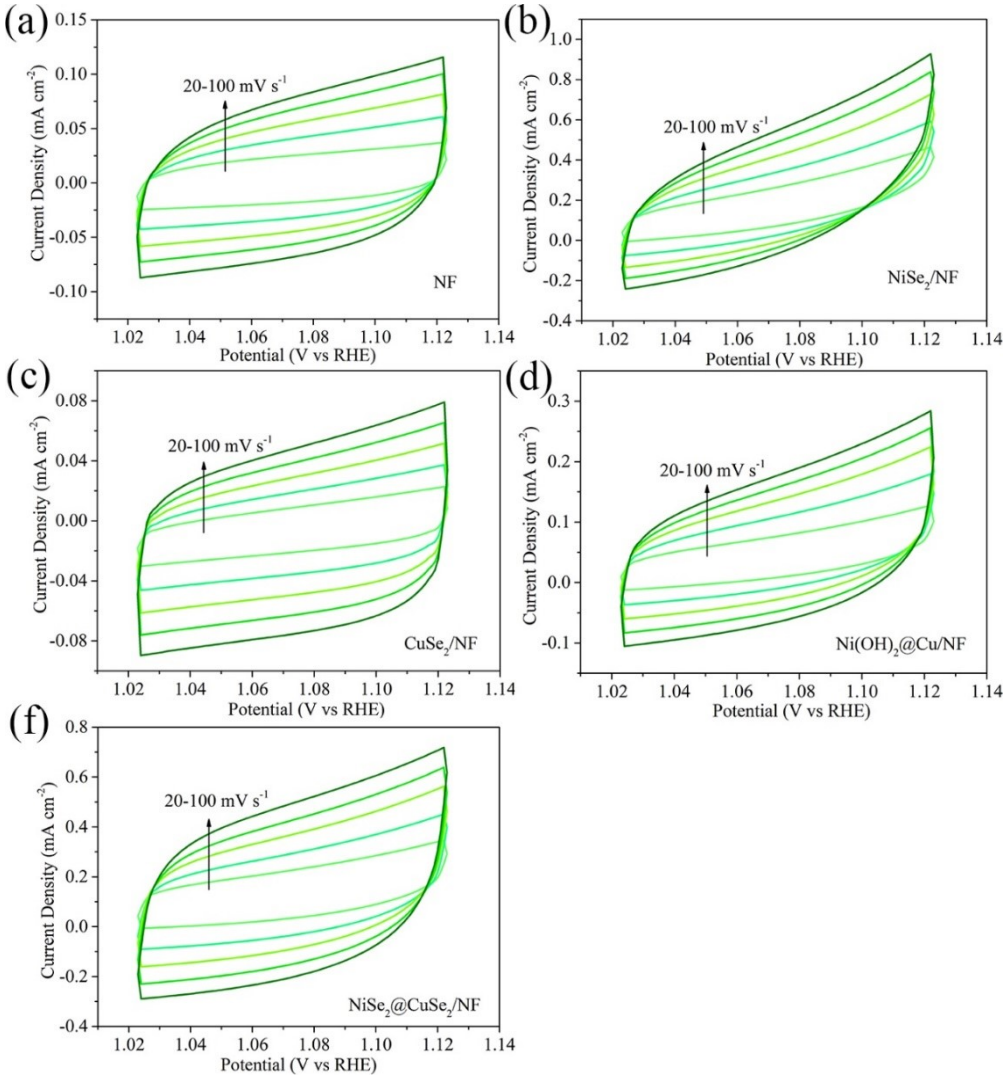

Fig. S10. CV curves at different scan rates for catalysts: a) NF, b) $NiSe_2$/NF, c) $CuSe_2$/NF, d) $Ni(OH)_2$@Cu/NF, and e) $NiSe_2$@$CuSe_2$/NF.

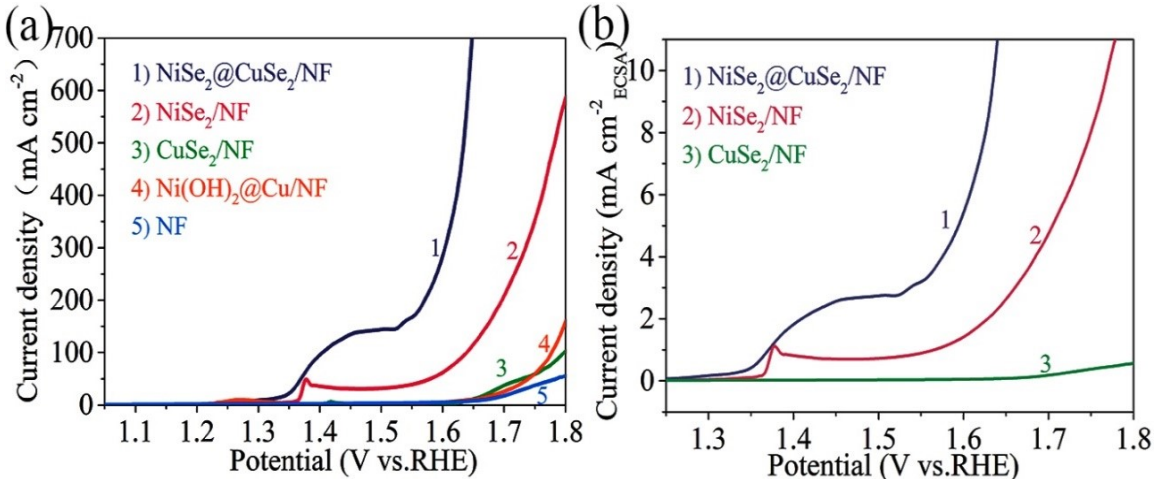

Fig. S11. a) LSV curves of $NiSe_2$@$CuSe_2$/NF, $NiSe_2$/NF, $CuSe_2$/NF, $Ni(OH)_2$@Cu/NF and NF after iR compensation. b) The OER performance of $NiSe_2$@$CuSe_2$/NF, $NiSe_2$/NF, and $CuSe_2$/NF after the electrochemical surface area normalization.

Table S3. TOFs of materials in this work.

Sample	$NiSe_2$@$CuSe_2$/NF	$NiSe_2$/NF	$CuSe_2$/NF	$Ni(OH)_2$/NF
n **(mol)**	2.25×10^{-5}	1.71×10^{-5}	1.67×10^{-5}	1.21×10^{-5}
j **(A cm^{-2})**	1.32×10^{-1}	5.15×10^{-2}	3.25×10^{-3}	1.31×10^{-2}
TOF (s^{-1})	7.58×10^{-3}	3.91×10^{-3}	2.52×10^{-4}	1.41×10^{-3}

TOFs are estimated by assuming that all the metal ions are active during the catalysis process. The current density is at the overpotential of 350 mV for materials. The equation of TOF = $(j \times S)/(4 \times F \times n)$ is utilized for OER calculation, where j is the current density (A cm^{-2}), S represents the surface area of as-prepared electrode, the number 4 means a four- electron reaction for OER. F is the Faraday constant (96485.3 C mol^{-1}), and n represents the moles of metal atoms on the electrode which can be calculated by the loading weight and the molecular weight of the catalyst.

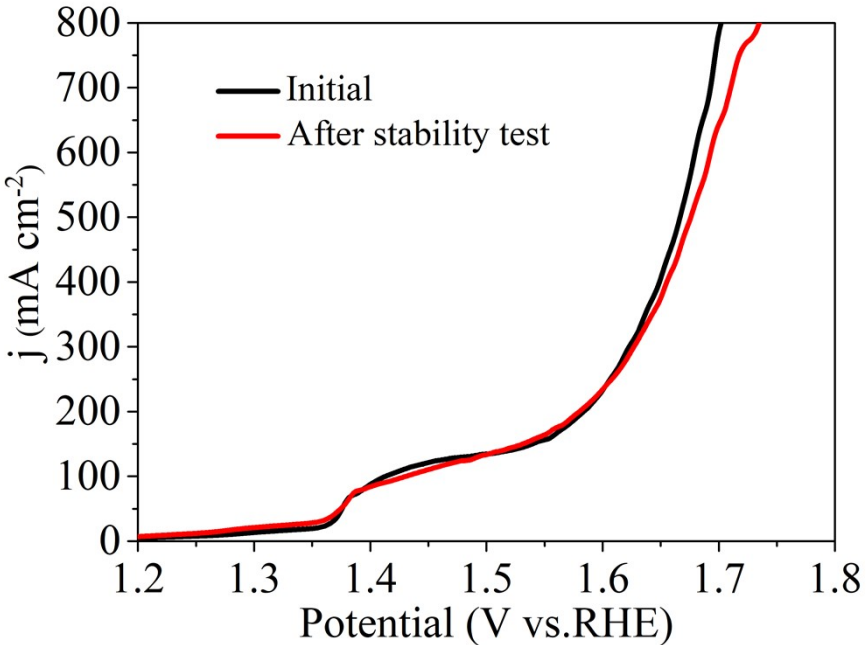

Fig. S12. LSV curves of $NiSe_2$@$CuSe_2$/NF before and after the test.

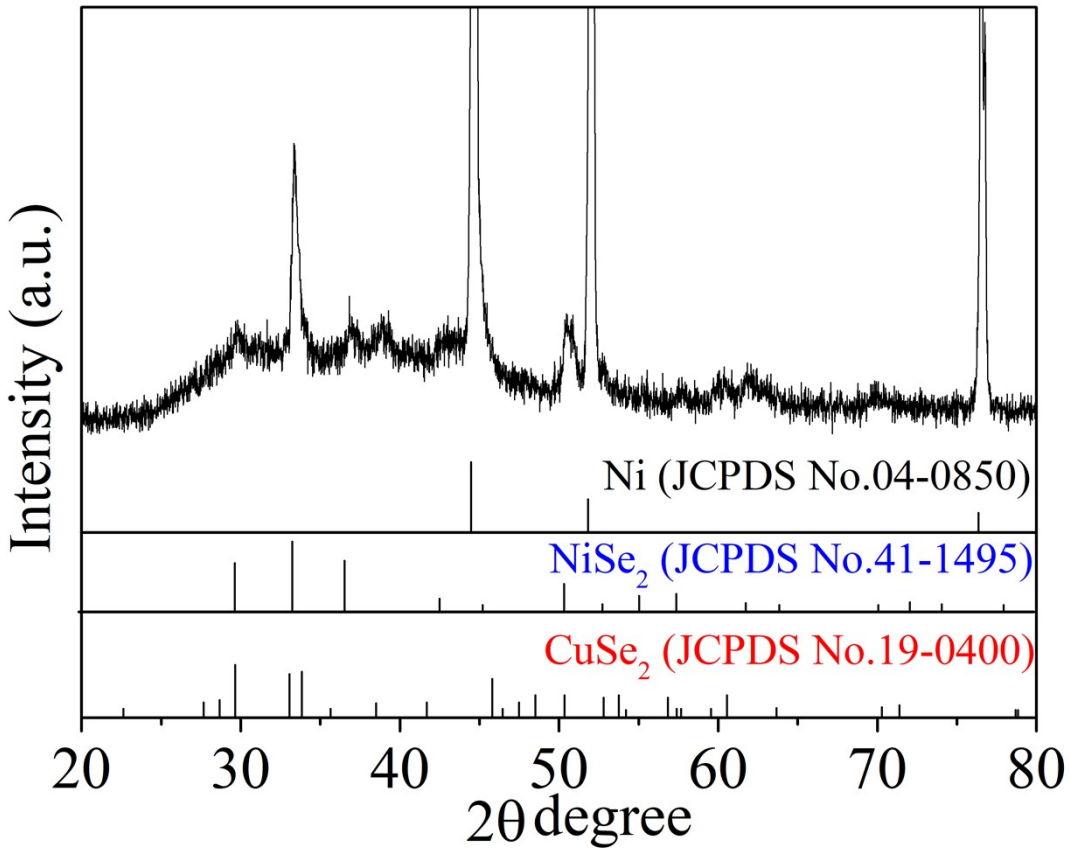

Fig. S13. XRD pattern of $NiSe_2$@$CuSe_2$/NF after test.

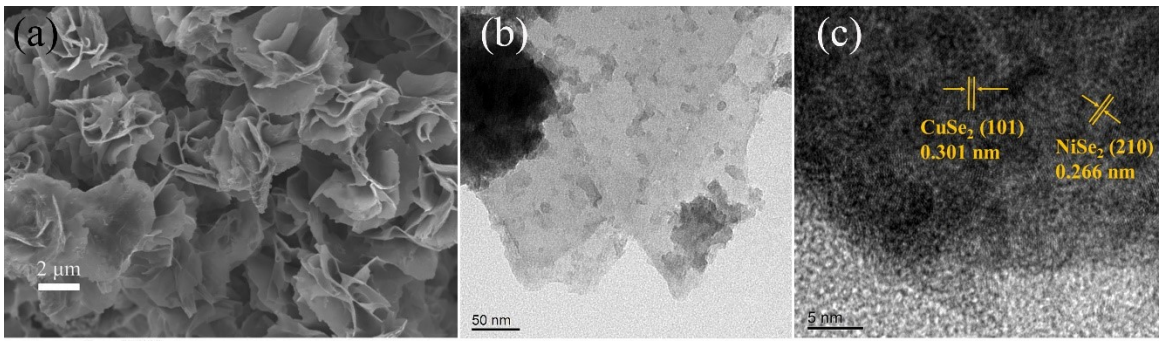

Fig. S14. a) SEM, b) TEM,and c) HRTEM images of $NiSe_2$@$CuSe_2$ after test.

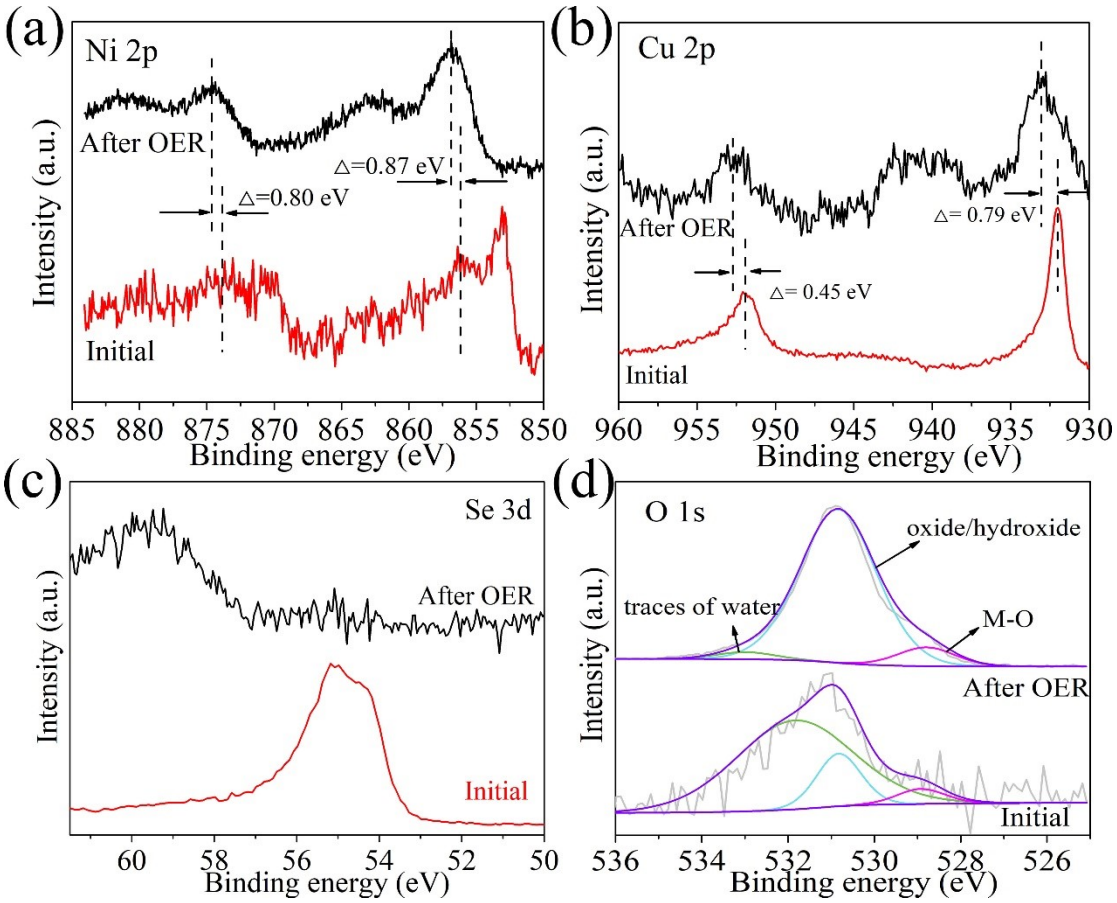

Fig. S15. The comparision of a) Ni 2p, b) Cu 2p spectrum, c) Se 3d spectrum and d) O 1s spectrum of $NiSe_2$@$CuSe_2$/NF before and after test.

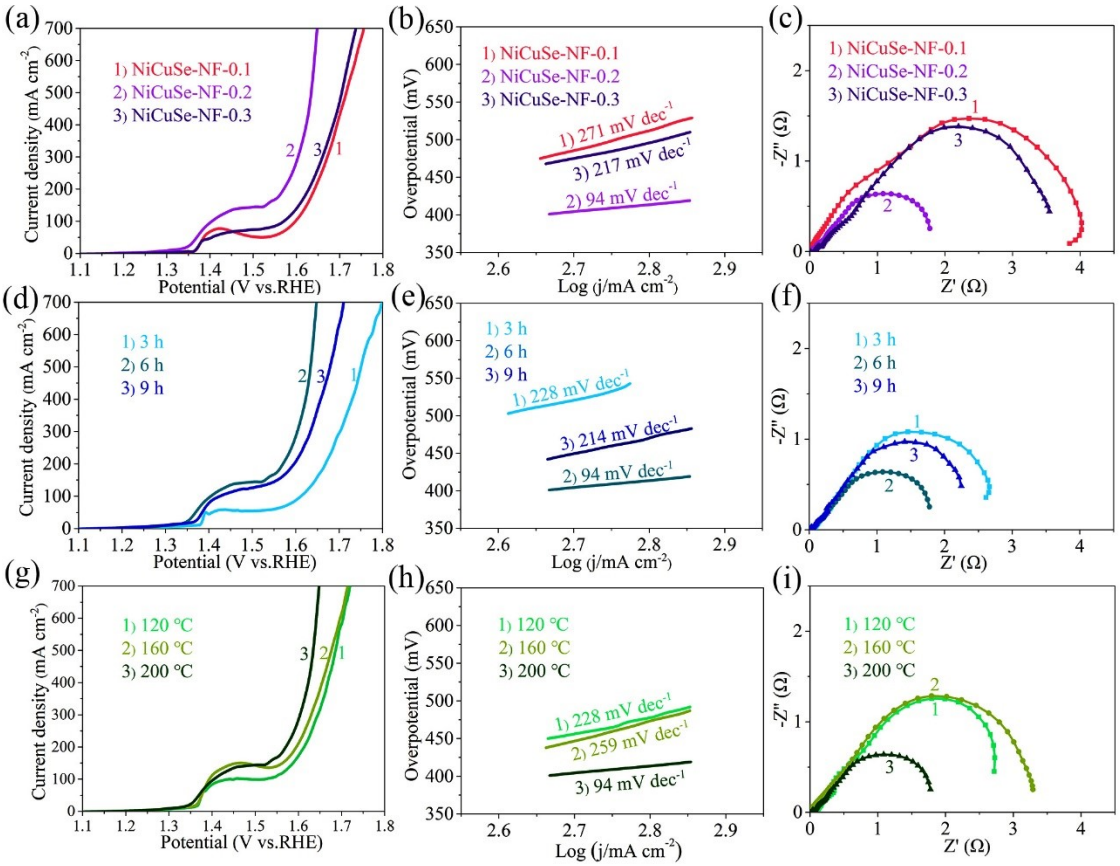

Fig. S16. a) OER polarization curves, b) Tafel slopes, c) Nyquist plots of NiCuSe-NF-0.1, NiCuSe-NF-0.2 and NiCuSe-NF-0.3. d) OER polarization curves, e) Tafel slopes, and f) Nyquist plots of different hydrothermal time (3 h, 6 h, 9 h). g) OER polarization curves, h) Tafel slopes, and i) Nyquist plots of different hydrothermal temperature (120 ^{o}C, 160 ^{o}C, 200 ^{o}C).

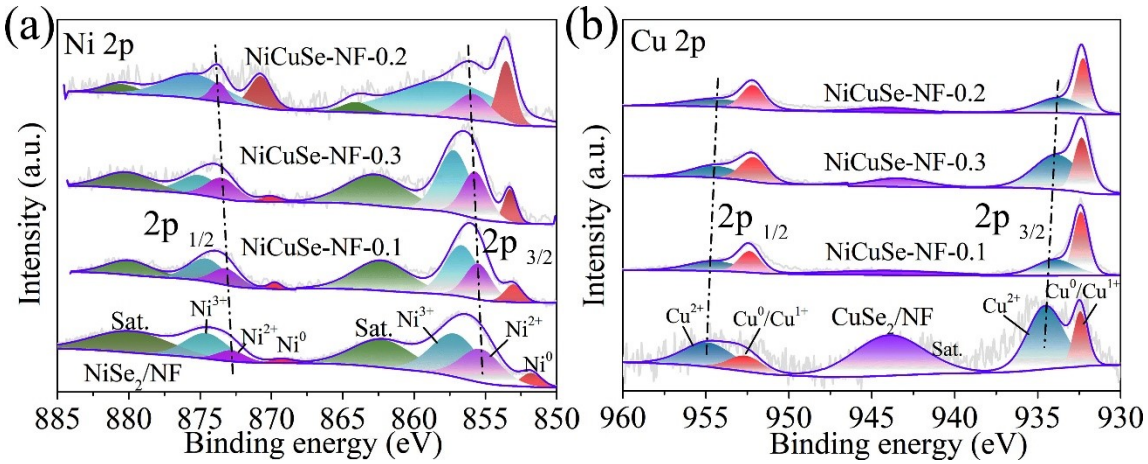

Fig. S17. a) Ni 2p spectra of $NiSe_2$/NF, NiCuSe-NF-0.1, NiCuSe-NF-0.2 and NiCuSe-NF-0.3. b) Cu 2p spectra of $CuSe_2$/NF, NiCuSe-NF-0.1, NiCuSe-NF-0.2 and NiCuSe-NF-0.3.

Table S4. The binding energies of Ni 2p of $NiSe_2$/NF, NiCuSe-NF-0.1, NiCuSe-NF-0.2, and NiCuSe-NF-0.3.

Sample	Ni 2p 3/2 (eV)			Ni 2p 1/2 (eV)		
	Ni^0	Ni^{2+}	Ni^{3+}	Ni^0	Ni^{2+}	Ni^{3+}
$NiSe_2$/NF	852.29	855.32	857.12	869.23	872.92	874.47
NiCuSe-NF-0.1	852.99	855.47	857.00	869.71	873.14	874.52
NiCuSe-NF-0.2	853.48	855.80	857.57	870.67	873.60	875.38
NiCuSe-NF-0.3	853.21	855.66	857.14	869.98	873.42	874.97

Table S5. The binding energies of Cu 2p of $CuSe_2$/NF, NiCuSe-NF-0.1, NiCuSe-NF-0.2, and NiCuSe-NF-0.3.

Sample	Cu 2p 3/2 (eV)		Cu 2p 1/2 (eV)	
	Cu^0/Cu^{1+}	Cu^{2+}	Cu^0/Cu^{1+}	Cu^{2+}
$CuSe_2$/NF	932.43	934.44	952.61	954.83
NiCuSe-NF-0.1	932.35	933.89	952.31	954.45
NiCuSe-NF-0.2	932.23	933.73	952.05	954.09
NiCuSe-NF-0.3	932.33	933.68	952.11	954.29

References

1 J. Zhou, Y. Liu, Z. Zhang, Z. Huang, X. Chen, X. Ren, L. Ren, X. Qi and J. Zhong, *Electrochim. Acta*, 2018, **279**, 195-203.

2 B. Chakraborty, R. Beltran-Suito, V. Hlukhyy, J. Schmidt, P. W. Menezes and M. Driess, *ChemSusChem*, 2020, **13**, 3222-3229.

3 X. Cao, J. E. Medvedeva and M. Nath, *ACS Appl. Energy Mater.*, 2020, **3**, 3092-3103.

4 L. Yang, L. Huang, Y. Yao and L. Jiao, *Appl. Catal. B Environ.*, 2021, **282**, 119584.

5 H. Liu, Z. Guo and J. Lian, *J. Solid State Chem.*, 2021, **293**, 121776.

6 G. Yilmaz, C. F. Tan, Y.-F. Lim and G. W. Ho, *Adv. Energy Mater.*, 2019, **9**, 1802983.

7 J. Yu, W.-J. Li, G. Kao, C.-Y. Xu, R. Chen, Q. Liu, J. Liu, H. Zhang and J. Wang, *J. Energy Chem.*, 2021, **60**, 111-120.

8 B. K. Kim, S.-K. Kim, S. K. Cho and J. J. Kim, *Appl. Catal. B Environ.*, 2018, **237**, 409-415.

9 J. Hou, Y. Sun, Z. Li, B. Zhang, S. Cao, Y. Wu, Z. Gao and L. Sun, *Adv. Funct. Mater.*, 2018, **28**, 1803278.

10 D. Chen, Z. Xu, W. Chen, G. Chen, J. Huang, C. Song, C. Li and K. Ostrikov, *J. Mater. Chem. A*, 2020, **8**, 12035-12044.

11 G. Wang, J. Huang, G. Chen, W. Chen, C. Song, M. Li, X. Wang, D. Chen, H. Zhu, X. Zhang and K. K. Ostrikov, *ACS Sustainable Chem. Eng.*, 2020, **8**,

17215-17224.

12 Y. Zhang, C. Zhang, Y. Guo, D. Liu, Y. Yu and B. Zhang, *J. Mater. Chem. A*, 2019, **7**, 2536-2540.

13 H. Ren, L. Yu, L. Yang, Z.-H. Huang, F. Kang and R. Lv, *J. Energy Chem.*, 2021, **60**, 194-201.

14 Y.-J. Tang, Y. Wang and K. Zhou, *J. Mater. Chem. A*, 2020, **8**, 7925-7934.

15 J. Zhou, L. Yuan, J. Wang, L. Song, Y. You, R. Zhou, J. Zhang and J. Xu, *J. Mater. Chem. A*, 2020, **8**, 8113-8120.